Supporting Information for Publication

Cancer cells invade confined microchannels via a self-directed mesenchymal-to-amoeboid transition

Andrew W Holle[a,b], Neethu Govindan Kutty Devi[a], Kim Clar[a,c], Anthony Fan[d], Taher Saif[d], Ralf Kemkemer†[a,c*], Joachim P Spatz†[a,b*]

[a] Department of Cellular Biophysics, Max Planck Institute for Medical Research, Heidelberg, Germany

[b] Department of Biophysical Chemistry, University of Heidelberg, Heidelberg, Germany

[c] Department of Applied Chemistry, Reutlingen University, Reutlingen, Germany

[d] Department of Mechanical Science and Engineering, University of Illinois at Urbana-Champaign, Urbana, IL, USA

Associated Content: Supporting Information/Materials and methods

Microchannel fabrication

Two-step photolithography was performed to fabricate the microchannel molds. Briefly, an 11 μm thick layer of SU-8 10 photoresist (MicroChem, Newton, MA, USA) was spincoated onto a silicon wafer (Siegert Wafer, Aachen, Germany) and crosslinked with UV light filtered through a photomask defining channel width at 3 and 10 μm (Compugraphics, Jena, Germany). This was repeated with SU-8 2075 (MicroChem, Newton, MA, USA) to form a 150 μm thick layer, with a second photomask defining channel length and reservoir area **(Fig. S4)**. Non-crosslinked photoresist was developed with mr-Dev 600 (Micro Resist Technology, Berlin, Germany). Polydimethylsiloxane (PDMS) (Dow Corning, Wiesbaden, Germany) was mixed at a 10:1 base to crosslinker ratio, centrifuged to remove bubbles, poured onto the silicon mold, and baked for four hours at 80 °C. This formulation has been shown to have a Young's modulus of approximately 2 MPa[1], which is nearly an order of magnitude stiffer than the extracellular matrix through which cancer cells would migrate (0.1-50 kPa)[2]. The PDMS was then peeled off the mold and cut into square chips with open reservoirs at the center and periphery. The PDMS chip and glass coverslips were treated with oxygen plasma (0.7 mbar, 300 W) for 25 seconds, brought into contact, and placed in an 80 °C oven for thirty minutes to facilitate irreversible binding. Type I collagen (100 μg/mL, Gibco, Carlsbad, CA, USA) or PBS (for experiments without ECM protein) was then added to the channels and incubated overnight at 4 °C.

Cell culture

MDA-MB-231, HS578T, BT549, MCF7, COLO205, LS178T, HCT8, and HCT116 cancer cell lines (ECACC, Salisbury, UK) (**Table S1**) were cultured in DMEM (31966, Gibco) supplemented with 10% FBS and 1% penicillin/streptomycin (100 µg/mL) (Life Technologies, Darmstadt, Germany). All experiments were performed in a 95% air/5% CO_2 mixture at 37 ^oC. SiR-Actin was used (Spirochrome, Stein am Rhein, Switzerland) for live cell imaging of the cytoskeleton. For inhibitor experiments, Y27632 dihydrochloride (p160ROCK) (LKT Laboratories, Hamburg, Germany) and NSC23766 (Rac1) (Santa Cruz Biotechnology, Dallas, TX, USA) were used at a concentration of 30 µM and 100 µM, respectively. At these concentrations, Y27632 has also been shown to inhibit protein kinase C (26 µM) and cAMP-dependent protein kinase (25 µM)[3]. NSC23766 functions as an inhibitor of Rac1-GEF interaction, but has also been shown to have off-target effects on acetylcholine inhibitors[4].

Microchannel invasion experiments

Chips were removed from 4 ^oC storage, rinsed in PBS, and glued to the bottom of a well in a six well plate with Picodent dental glue (Picodent, Wipperfürth, Germany). Sterilization was performed for 25 minutes under UV light. Cells were trypsinized and resuspended to a density of 1 x 10^6 cells/mL. 100 µL (100,000 cells) of the cell solution was added to the center chamber of the invasion chip. While the center of the chip is open to the atmosphere, the reservoirs are approximately 150 µm tall, confining the volume of cell solution in front of the channels to approximately 60 nL. This quantity of cells was chosen in order to introduce enough cells to encourage channel interactions but not so many

that cell-cell interactions began to influence migration. Cells were allowed to attach for one hour before the entire well was filled with media and the samples were transferred to the microscope. As the heights of the media column above both the inside and outside regions of the chip are equal, no hydrostatic pressure induced fluid flow is possible. For inhibitor experiments, the inhibitor was added one hour after the cells. For experiments in which channels were used without ECM proteins, cells were resuspended in FBS-free DMEM to prevent non-specific protein adsorption in the channels. Phase contrast live-cell imaging was performed in a cell culture chamber built around an Axiovert 200M inverted microscope with a motorized stage (Carl Zeiss, Jena, Germany). Images were collected every ten minutes from up to 50 fields of view per experiment for 24 hours.

For experiments utilizing the SiR series of live cell dyes, the cell-permeable dye was introduced to cells at a concentration of 100 nM (SiR-Actin) and allowed to incubate for 6 hours before imaging. Live cell fluorescent imaging was performed with an LSM 880 confocal laser scanning microscope (Zeiss).

Image analysis

Image sequences were analyzed in Fiji (NIH)[5] using the manual tracking plugin to identify the position of the leading edge of permeating cells that were fully within the channel. Data obtained from image analysis was analyzed in Microsoft Excel, with instantaneous cell speeds calculated for each 10-minute increment and average cell speeds calculated by averaging the average speeds of each cell. Cells were grouped within three characteristic categories: *penetrative* cells were those that sent protrusions at least 10 μm into a channel, *invasive* cells were those that sent protrusions at least 75 μm into the channel

or fully entered, and *permeative* cells were those that entered and subsequently exited the opposite side of the channel. Cell speeds were only calculated for cells that fully permeated a channel. The method for tracking cell permeation involved identifying a permeative cell, rewinding the movie to find when it began the permeative process, then tracking the position of the leading edge until the it exited the channel. As some cells spent extended amounts of time interacting with the channel entrance prior to the permeative event, some measurements began when the cell's leading edge was already 5-10 microns into the channel. For cells that had already started the permeative process at the beginning of the video, the event was analyzed as long as the leading edge was not farther than 50 μm into the channel. Kymographs of permeating cells were constructed in Fiji. All images displayed in figures for comparison are scaled identically.

Immunofluorescence

Cells were fixed in 3.7% formaldehyde for 15 minutes and permeabilized in 0.1% Triton X-100. Cells were then stained with primary antibodies against human paxillin (ab32084, Abcam, Cambridge, UK) and β1 integrin (MAB17781, Millipore, Burlington, MA, USA). Corresponding secondary antibodies were conjugated to Alexa Fluor 488 (FITC) or Alexa Fluor 647 (Cy5) (Life Technologies, Carlsbad, CA, USA). Nuclei were counterstained with Hoechst dye (Thermo Scientific, Rockford, IL, USA) and actin was stained with Alexa Fluor 568 Phalloidin (Life Technologies). For integrin β1 imaging, cells were permeabilized in a 0.5% Saponin in PBS solution for 10 minutes at room temperature to prevent membrane solubilization, non-selective protein extraction, and false negatives[6].

To image protein adsorption, empty channels conjugated with ECM proteins were stained with primary antibodies against human collagen (ab34710, Abcam).

Statistical Analysis

Data analysis was performed in Microsoft Excel and Graphpad Prism. At least 3 independent replicates were performed for each experiment. Technical repeats in the form of both multiple chips observed per experiment and multiple positions recorded from each chip were also performed. Sample sizes are indicated in figure captions. Two-tailed Student's t tests were used when only two populations were compared. One-way ANOVA was utilized to compare multiple population means when multiple comparisons were required, with individual post hoc comparisons performed with Sidak's multiple comparisons test.

Supplemental Figures

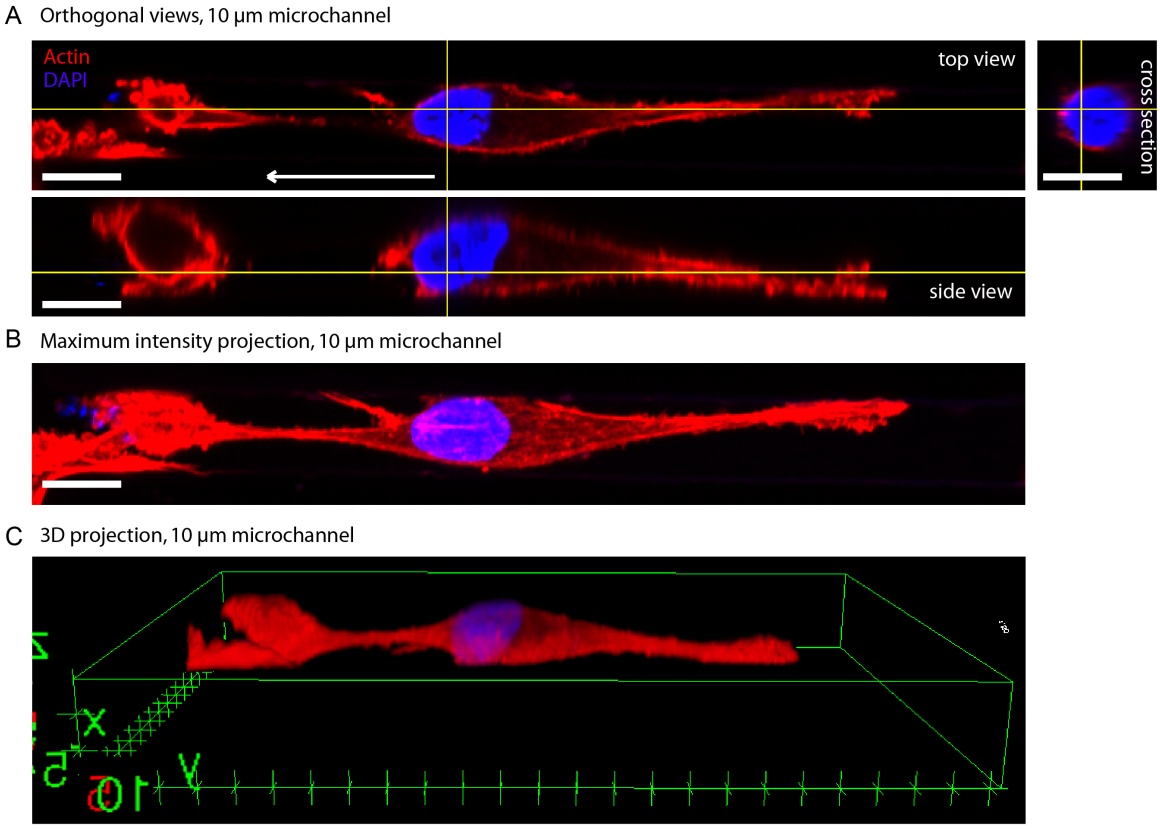

Figure S1: Three dimensional projections of an MDA-MB-231 breast cancer cell in a 10 µm microchannel. A) Top, side, and cross sectional orthogonal slices are shown. Scale bars=10 µm for all projections. **B)** Top view of maximum intensity projection. Scale bar=10 µm. C) Rotated 3D projection.

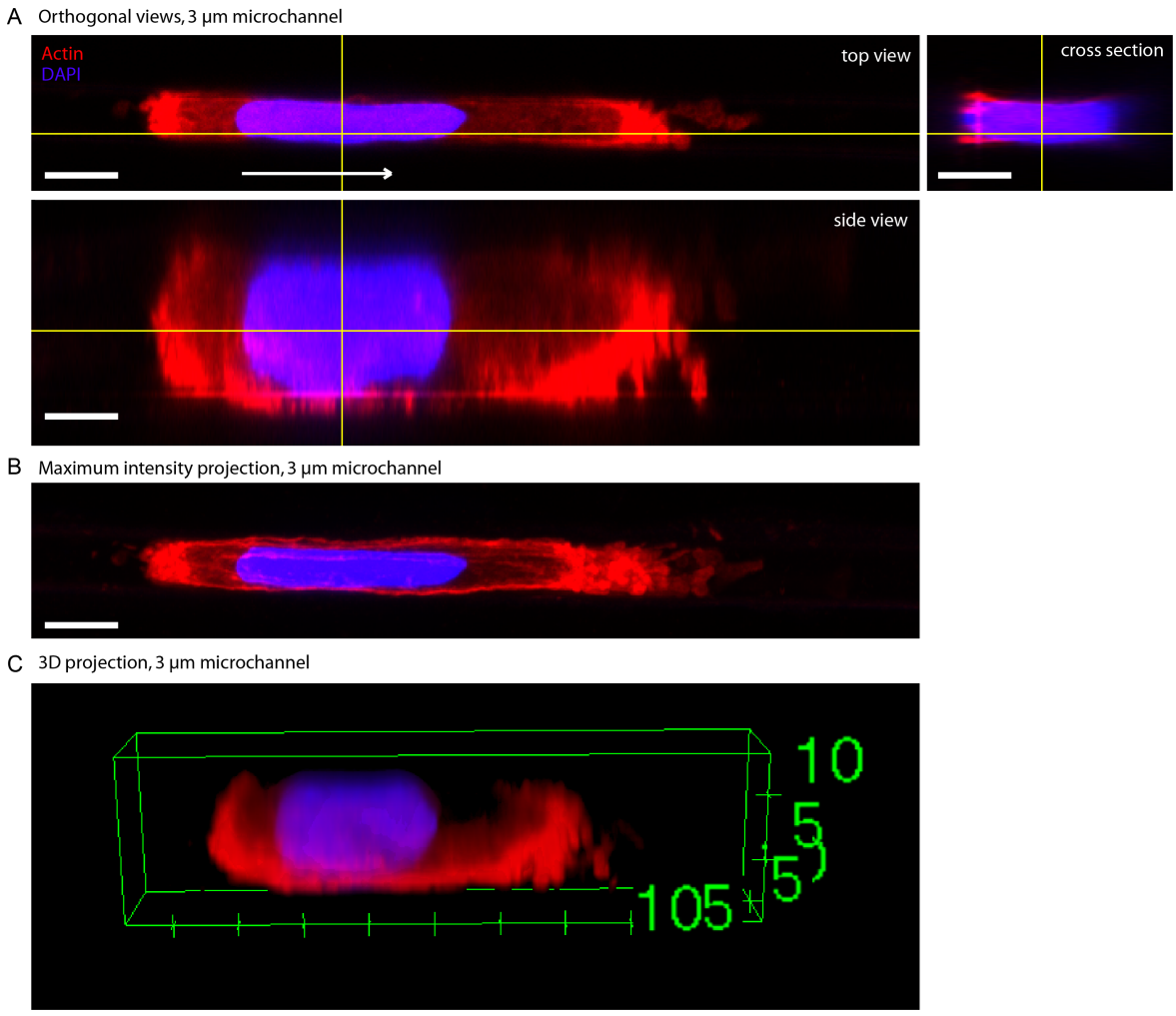

Figure S2: Three dimensional projections of an MDA-MB-231 breast cancer cell in a 3 µm microchannel. A) Top, side, and cross sectional orthogonal slices are shown. Scale bars=5 µm for all projections. **B)** Top view of maximum intensity projection. Scale bar=5 µm. C) Rotated 3D projection.

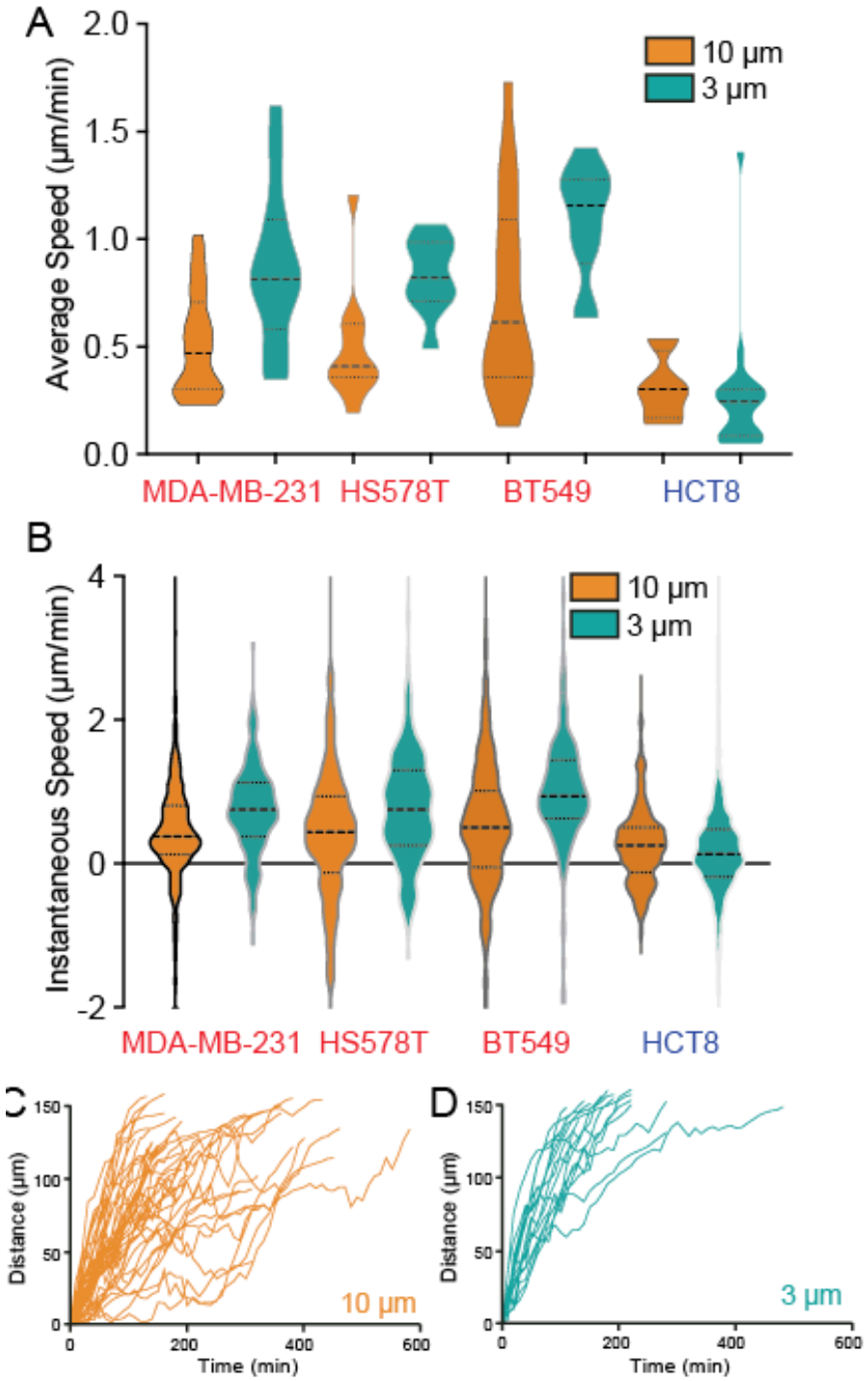

133

134 **Figure S3:** Violin plots of the A) average cell speed and B) instantaneous cell velocity

135 measured across four different permeative cell lines. C-D) Individual traces of leading

136 edge position over time in 10 µm and 3 µm channels.

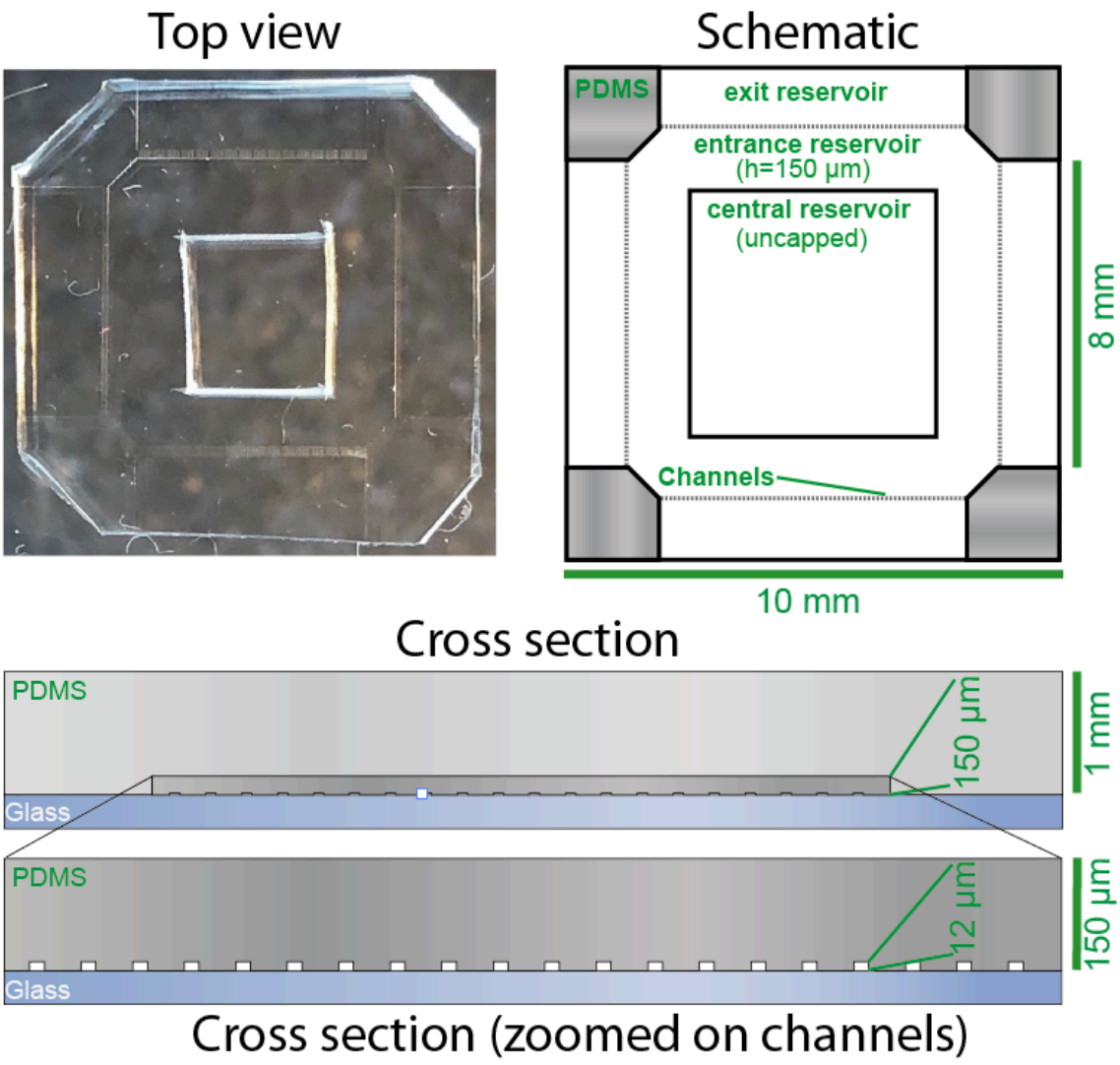

137

138 **Figure S4:** A picture and schematic of the microchannel chip

139

Supplemental Video Captions

Video S1: Phase contrast time lapse imaging of an MDA-MB-231 cell permeating a 3 μm channel. Bleb structures are observed upon channel exit. This video is displayed at 10 frames per second with each frame representing 10 minutes.

Video S2: Phase contrast time lapse imaging of an HS578T cell permeating a 3 μm channel. Bleb structures are observed upon channel exit. This video is displayed at 10 frames per second with each frame representing 10 minutes.

Video S3: Phase contrast time lapse imaging of a BT549 cell permeating a 3 μm channel. Bleb structures are observed upon channel exit. This video is displayed at 10 frames per second with each frame representing 10 minutes.

Video S4: Phase contrast time lapse imaging of an HCT-8 cell permeating a 3 μm channel. Bleb structures are observed upon channel exit. This video is displayed at 10 frames per second with each frame representing 10 minutes.

Video S5: Maximum intensity projection of a confocal time lapse image of an SiR-Actin labeled MDA-MB-231 cell moving through a 10 μm channel. This video is displayed at 10 frames per second with each frame representing 10 minutes.

Video S6: Maximum intensity projection of a confocal time lapse image of an SiR-Actin labeled MDA-MB-231 cell moving through a 3 μm channel. This video is displayed at 10 frames per second with each frame representing 10 minutes.

Video S7: Phase contrast time lapse imaging of MDA-MB-231 cells in a protein-free PDMS chip with 10 μm widths in 0% FBS media. This video is displayed at 10 frames per second with each frame representing 10 minutes.

Video S8: Phase contrast time lapse imaging of MDA-MB-231 cells in a protein-free PDMS chip with 3 μm widths in 0% FBS media. This video is displayed at 10 frames per second with each frame representing 10 minutes.

Video S9: Phase contrast time lapse imaging of an MCF-7 cell in a 10 μm channel. MCF-7 cells do not permeate 3 μm channels. This cell displays amoeboid characteristics while permeating the wide 10 μm channel. This video is displayed at 10 frames per second with each frame representing 10 minutes.

Video S10: Phase contrast time lapse imaging of MDA-MB-231 cells in a 10 μm channel. One cell permeates the microchannel, then re-enters a different microchannel

and migrates back towards the cell reservoir. This video is displayed at 10 frames per second with each frame representing 10 minutes.

Video S11: Phase contrast time lapse imaging of MDA-MB-231 cells in a 3 μm channel displaying contact guidance along the edges of the chip after exiting. This video is displayed at 10 frames per second with each frame representing 10 minutes.

Cell line	*Tissue*	*Disease*	*Tumorigenic*	*Invasive*	*Cell type*	*Citation*	*Receptors*	*Notes*
MDA-MB-231	Breast	Invasive ductal carcinoma	Yes	Yes	Epithelial	[7,8]	Triple negative	Claudin-low
Hs578T	Breast	Carcinosarcoma	Yes	Yes	Epithelial	[7,9]	Triple negative	Claudin-low
BT549	Breast	Invasive ductal carcinoma	Yes	Yes	Epithelial	[7,8]	Triple negative	Claudin-low
MCF-7	Breast	Invasive ductal carcinoma	Yes	No	Epithelial	[7,10]	HER2-	Luminal A
COLO 205	Colon	Colorectal adenocarcinoma	Yes	High	Epithelial	[11,12]		
HCT-8	Colon	Colorectal adenocarcinoma	Yes	Low	Epithelial	[13-15]		
HCT-116	Colon	Colorectal carcinoma	Yes	Low	Epithelial	[13,16]		
LS174T	Colon	Colorectal adenocarcinoma	Yes	Mid	Epithelial	[14,17]		

Table S1: Cell lines used in microchannel invasion assay. Characterization of tumorigenesis and invasiveness can vary based on experimental protocol. For example, HCT-8 colorectal cancer cells have been shown to not be tumorigenic in spleens and livers of nude mice[14], but were found to generally tumorigenic in nude mice in a different study[15]. Low, middle, and high levels of invasiveness are often comparative metrics and can also vary across experimental systems (through Matrigel, collagen matrices, or Boyden chamber pores). Descriptions of receptor expression and further characterizing features are given for breast cancer cell lines.

References (Supplemental Material)

(1) Johnston, I. D.; McCluskey, D. K.; Tan, C. K. L.; Tracey, M. C. *J. Micromech. Microeng.* **2014**, *24* (3), 035017.

(2) Holle, A. W.; Van Vliet, K. J.; Kamm, R. D.; Discher, D.; Janmey, P.; Saif, T. *Nano Lett.* **2017**, *18* (1), 1–8.

(3) Uehata, M.; Ishizaki, T.; Satoh, H.; Ono, T. *Nature* **1997**.

(4) Levay, M.; Krobert, K. A.; Wittig, K.; Voigt, N.; Bermudez, M.; Wolber, G.; Dobrev, D.; Levy, F. O.; Wieland, T. *J Pharmacol Exp Ther* **2013**, *347* (1), 69–79.

(5) Schindelin, J.; Arganda-Carreras, I.; Frise, E.; Kaynig, V.; Longair, M.; Pietzsch, T.; Preibisch, S.; Rueden, C.; Saalfeld, S.; Schmid, B.; Tinevez, J.-Y.; White, D. J.; Hartenstein, V.; Eliceiri, K.; Tomancak, P.; Cardona, A. *Nature Methods* **2012**, *9* (7), 676–682.

(6) Jamur, M. C.; Oliver, C. In *Immunocytochemical Methods and Protocols*; Methods in Molecular Biology; Humana Press: Totowa, NJ, 2010; Vol. 588, pp 63–66.

(7) Evtimova, V.; Zeillinger, R.; Weidle, U. H. *Tumor Biol.* **2003**, *24* (4), 189–198.

(8) Tate, C. R.; Rhodes, L. V.; Segar, H. C.; Driver, J. L.; Pounder, F. N.; Burow, M. E.; Collins-Burow, B. M. *Breast Cancer Res.* **2012**, *14* (3).

(9) Daniel, J.; Coulter, J.; Woo, J.-H.; Wilsbach, K.; Gabrielson, E. *PNAS* **2011**, *108* (13), 5384–5389.

(10) Shafie, S. M.; Liotta, L. A. *Cancer Letters* **1980**, *11* (2), 81–87.

(11) de Toledo, M.; Anguille, C.; Roger, L.; Roux, P.; Gadea, G. *PLoS ONE* **2012**, *7* (11), e48344.

(12) Senger, D. R.; Perruzzi, C. A. *Cancer Research* **1985**, *45* (11), 5818–5823.

(13) Vermeulen, S. J.; Bruyneel, E. A.; Bracke, M. E.; Debruyne, G. K.; Vennekens, K. M.; Vleminckx, K. L.; Berx, G. J.; Vanroy, F. M.; Mareel, M. M. *Cancer Research* **1995**, *55* (20), 4722–4728.

(14) Tibbetts, L. M.; Doremus, C. M.; Tzanakakis, G. N.; Vezeridis, M. P. *Cancer* **1993**, *71* (2), 315–321.

(15) Rosenthal, K. L.; Tompkins, W.; Frank, G. L.; McCulloch, P.; Rawls, W. E. *Cancer Research* **1977**, *37* (11), 4024–4030.

(16) Zhu, F.; Zykova, T. A.; Kang, B. S.; Wang, Z.; Ebeling, M. C.; Abe, Y.; Ma, W. Y.; Bode, A. M.; Dong, Z. *Gastroenterology* **2007**, *133* (1), 219–231.

(17) Brabletz, T.; Jung, A.; Reu, S.; Porzner, M.; Hlubek, F.; Kunz-Schughart, L. A.; Knuechel, R.; Kirchner, T. *PNAS* **2001**, *98* (18), 10356–10361.